Acta Mech 228, 1071–1081 (2017)
DOI 10.1007/s00707-016-1744-9

ORIGINAL PAPER

Hamdi Ezzin · Morched Ben Amor · Mohamed Hédi Ben Ghozlen

Propagation behavior of SH waves in layered piezoelectric/piezomagnetic plates

Received: 4 January 2016 / Revised: 5 July 2016 / Published online: 17 November 2016

Abstract The propagation of shear horizontal waves in laminated piezomagnetic/piezoelectric plates was investigated using the ordinary differential equation and stiffness matrix methods. Commonly used materials, namely barium titanate as piezoelectric 'B' and cobalt ferrite as piezomagnetic 'F', were retained for illustration. The dispersion curves of the first five modes were shown for different sequences F/F, B/B, and F/B. The effects of thickness ratio on phase and group velocities as well as the influence on the magneto-electromechanical coupling factor of the first mode were investigated. Large magneto-electromechanical coupling factors could be achieved by an appropriate adjustment of the thickness ratio. The present investigation is of practical interest for developing new layered composites made of smart piezoelectric and piezomagnetic devices for engineering applications.

1 Introduction

In recent years, magnetic and electronic materials have received much attention with their increasing use in engineering applications including sensors and actuators. However, combining ferromagnetism and ferroelectricity in the same phase has proven to be surprisingly difficult at the atomic level. Indeed, studies, including the manufacture of several kinds of multiferroic composite materials consisting of piezoelectric (PE) and piezomagnetic (PM) phases [1–3], have been undertaken to overcome these difficulties. These composites have a magnetoelectric effect that is not present in single-phase PE or PM material. The laminated magnetoelectric materials (ME) show a high coupling coefficient, indicating great potential for resonators, sensors, and energy harvesters, etc. It is therefore useful to understand the mechanical behavior of ME materials in depth and analyze the physical quantities involved in coupling. Wave problems on PE/PM structures have been widely investigated [4]. In terms of methodology for solving problems in layered systems, the propagator matrix and the state vector approaches are the most popular methods, among others (e.g., Thomson [5], Haskell [6], Gilbert and Backus [7], Bahar [8]). Due to their conceptual simplicity, reduced programming effort and computing time, these approaches have now been extended to various complicated layered structures, including static, free vibration analysis, and magnetoelectric coupling behavior of magneto-electroelastic materials [9–11]. Jiangong et al. [12] studied dispersion relations of waves in multilayered magneto-electroelastic plates. Other studies have investigated horizontal shear waves (SH) at the interface of two magneto-electroelastic half-spaces [13]. Love waves in a PE/PM layered structure [14] or layered magneto-electroelastic structure with

H. Ezzin (✉) · M. H. B. Ghozlen
Laboratory of Physics of Materials, Faculty of Sciences of Sfax, University of Sfax, BP 1171, 3000 Sfax, Tunisia
E-mail: ezzinhamdi@yahoo.fr
Tel.: (+216) 52 389 058; (+216) 29 037 859

M. B. Amor
Sfax Preparatory Engineering Institute, Menzel Chaker Road 0.5 km, BP 1172, 3000 Sfax, Tunisia

initial stress were also published [15]. In these reports the material in the layered structure should be considered as homogeneous material in each layer. Chen and Chen investigated the Love wave behavior in a magneto-electroelastic multilayered structure by the propagation matrix method [16]. Using the propagator matrix and the state vector approaches, an analytical treatment was presented for the propagation of harmonic waves in magneto-electroelastic plates by Chen et al. [17]. SH wave propagation in a layered system consisting of a layer bonded to a different semi-infinite substrate is of intensive research interest in recent years. Wang et al. [18] studied the love wave propagation in a PE lamina bonded into a semi-infinite metal medium. They conclude that the phase velocities initiated at the shear wave velocity of the host medium tend toward the Bleustein Gulyaev surface wave velocity for the PE layer at high wave numbers for the first mode. In their studies, Fan and Yang [19] analyzed the propagation behavior of SH surface waves in a layered system consisting of a PE half-space and a metal or elastic dielectric layer with an imperfect interface. They found that the dispersion characteristics were sensitive to the interface properties. The objective of this work is to study the SH waves propagation in layered PE/PM plate. For that purpose the stiffness matrix method (SMM) and the ordinary differential equation (ODE) [20,21] have been extended to the study of the magneto-electroelastic multilayered structure. The constitutive relations used are of general anisotropy, which possess simultaneously the coupling effects between mechanical, electric and magnetic fields. Numerical examples are presented to show the features of dispersion curves for different sequences F/F, B/B and F/B. Furthermore, the effect of the thickness ratio of the PE layer to the PM layer on phase and group velocities are studied for the first mode.

2 Statement of the problem

Consider a PM layer perfectly bonded to a PE layer, their thicknesses denoted by $h^{\mathrm{m}}, h^{\mathrm{e}}$ respectively, as illustrated in Fig. 1. Both materials are hexagonal (6 mm crystals) and polarized along the x_2 axis. The (x_1, x_3) plane is an isotropic plane for both materials. We are interested in SH-guided waves propagating in the (x_1, x_3) plane, the anti-plane acoustic mode and the in-plane electromagnetic mode are coupled. The constitutive equations for the PM and PE layers can be expressed as follows [21,22].

For an anisotropic and linearly magneto-electroelastic solid, the coupled constitutive relation can be written as:

$$\tau_{ij} = C_{ijkl}\frac{\partial u_k}{\partial x_l} - e_{kij}E_k - q_{kij}H_k, \tag{1}$$

$$D_i = e_{ikl}\frac{\partial u_k}{\partial x_l} + \varepsilon_{ik}E_k, \tag{2}$$

$$B_i = q_{ikl}\frac{\partial u_k}{\partial x_l} + \mu_{ik}H_k, \tag{3}$$

$$E_i = -\phi_{,i},\ H = -\psi_{,i}, \tag{4}$$

where τ_{ij}, D_i and B_i, E_i, H_i and u_i are the components of the stress tensor, the electric displacement, the magnetic induction, the electric field, the magnetic field, and the particle displacement, respectively. Here, and throughout the article, Einstein's summation convention is used, and i, j, k and $l = 1, 2, 3$ or equivalently x, y, z. C_{ijkl}, e_{ijk}, q_{ijk}, ε_{ij} and μ_{ik} are material parameters, i.e., the elastic constants, the piezoelectric constants, the piezomagnetic constants, the dielectric permittivity constants, and the magnetic permeability constants, respectively. Here, the magneto-electric coupling constant is not considered.

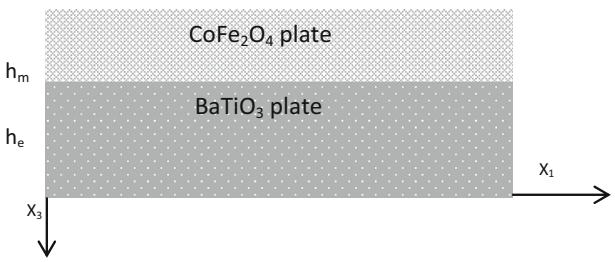

Fig. 1 Geometry of multiferroic laminate

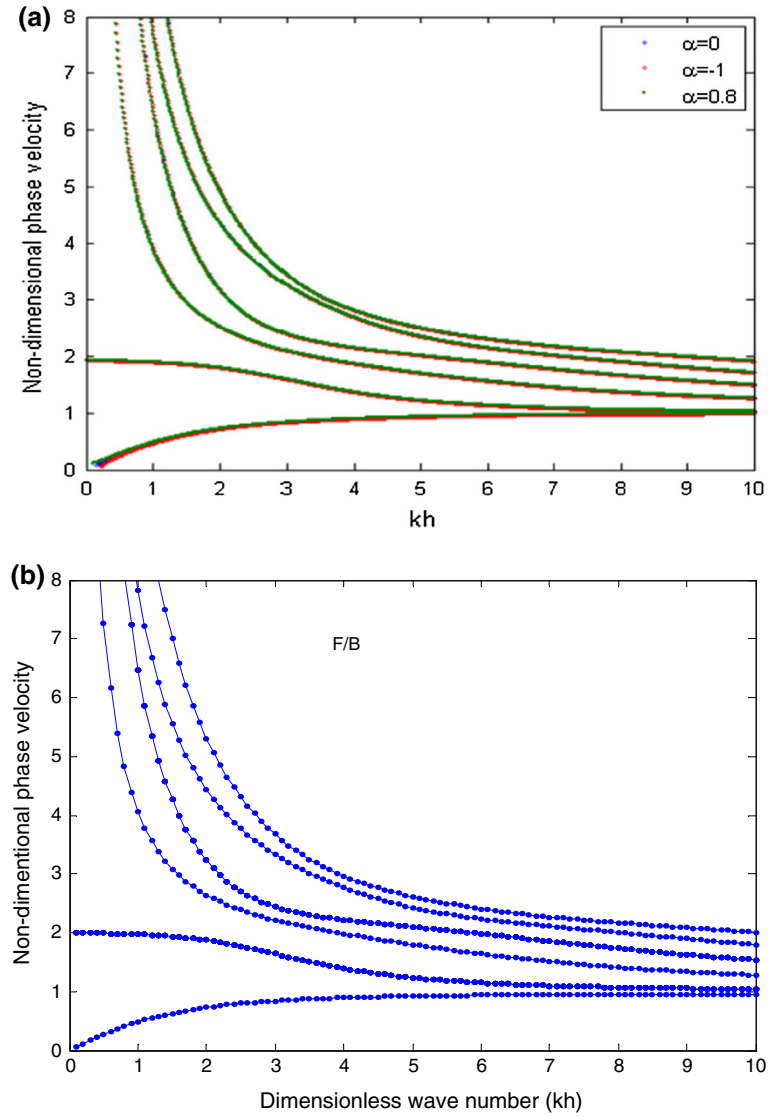

Fig. 2 Dispersion curves of the PM/PE laminate. **a** Result from [25]. **b** Obtained result

For an orthotropic solid, with transverse isotropy being a special case, the material coefficients in Eq. (1) can be written as:

$$[C] = \begin{bmatrix} C_{11} & C_{12} & C_{13} & 0 & 0 & 0 \\ & C_{22} & C_{23} & 0 & 0 & 0 \\ & & C_{33} & 0 & 0 & 0 \\ & & & C_{44} & 0 & 0 \\ & Sym & & & C_{55} & 0 \\ & & & & & C_{66} \end{bmatrix}, \quad [e] = \begin{bmatrix} 0 & 0 & e_{31} \\ 0 & 0 & e_{32} \\ 0 & 0 & e_{33} \\ 0 & e_{24} & 0 \\ e_{15} & 0 & 0 \\ 0 & 0 & 0 \end{bmatrix}, \quad [q] = \begin{bmatrix} 0 & 0 & q_{31} \\ 0 & 0 & q_{32} \\ 0 & 0 & q_{33} \\ 0 & q_{24} & 0 \\ q_{15} & 0 & 0 \\ 0 & 0 & 0 \end{bmatrix},$$

$$[\varepsilon] = \begin{bmatrix} \varepsilon_{11} & 0 & 0 \\ 0 & \varepsilon_{22} & 0 \\ 0 & 0 & \varepsilon_{33} \end{bmatrix}, \quad [\mu] = \begin{bmatrix} \mu_{11} & 0 & 0 \\ 0 & \mu_{22} & 0 \\ 0 & 0 & \mu_{33} \end{bmatrix},$$

where $u_i = (u_1, u_2, u_3)^{\mathrm{T}}$, ϕ and ψ are the elastic displacement, electric potential and magnetic potential, respectively.

For the wave propagation considered in this paper, the body forces, electric charge, and current density are assumed to be zero. Thus, the dynamic equation for the magneto-electro-elastic media is governed by

$$\tau_{ij,j} = \rho \frac{\partial^2 u_i}{\partial t^2}, \tag{5}$$

$$D_{j,j} = 0, \tag{6}$$

$$B_{j,j} = 0, \tag{7}$$

where ρ is the density of the material.

3 Solutions of the problem

On the assumption of a harmonic wave propagating in x_1 direction, the solutions to Eq. (8) can be expressed as $\xi(x_3) = \xi(x_3)\exp(i\,(k_1 x_1 - \omega t))$. The wave equation is written under the Thomson-Haskell parameterization of the Stroh formalism [5,6]:

$$\frac{\mathrm{d}}{\mathrm{d}x_3}\xi(x_3) = -i\omega\, Q\, \xi(x_3), \tag{8}$$

where $\xi(x_3) = [-i\omega U,\, T]^{\mathrm{T}}$ represents the state vector including ten components. Thus, the set of components can be detailed: $U = [u_i,\ \phi,\ \psi]^{\mathrm{T}}$ and $T = [\tau_{i3},\ D_3,\ B_3]^{\mathrm{T}}$ with $i = 1, 2,$ and 3.

The generalized stress vector T consists of the mechanical stress vector τ_{i3}, the normal electric displacement component D_3 and the normal magnetic induction component B_3. In the same way, the generalized displacement vector U includes the mechanical displacement components u_i, the electrical potential ϕ and the magnetic potential ψ. For the transverse configuration, the displacement component u_2, the electrical potential ϕ, and the magnetic potential ψ are uncoupled from the sagittal components (u_1, u_3). Q, known as the fundamental acoustic tensor "fat" [23,24], is a (6×6) square matrix which depends mainly on the physical properties and the guiding slowness component S_1.This configuration is advantageous, since it excludes, for Q, any dependency of the angular frequency ω, and it is given by:

$$Q = -i\omega \begin{bmatrix} S_1\Gamma_{33}^{-1}\Gamma_{31} & \Gamma_{33}^{-1}. \\ S_1^2(\Gamma_{13}\Gamma_{33}^{-1}\Gamma_{31} - \Gamma_{11}) + \rho I_3 & S_1\Gamma_{13}\Gamma_{33}^{-1} \end{bmatrix}. \tag{9}$$

Γ_{ik} are the (3×3) matrices formed from the elastic constants C_{ijkl}, piezoelectric constant e_{ijk}, piezomagnetic constants q_{ijk}, dielectric permittivity ε_{ij} and magnetic permeability constants μ_{ik}:

$$\Gamma_{ik} = \begin{bmatrix} C_{2i2k} & e_{k2i} & q_{k2i} \\ e_{i2k} & -\varepsilon_{ik} & 0 \\ q_{i2k} & 0 & -\mu_{ik} \end{bmatrix}.$$

For the sake of brevity, this classical procedure which permits to obtain the guiding wave number and the phase velocity is not given in details. However, it should be recalled that because of the anisotropy and the complexity of the problem, the dispersion equations can only be solved numerically. In addition, the solution associated with SH wave propagation must satisfy the boundary conditions on the inner interface and the free surfaces. The continuity conditions at the interface between the PM/PE layers are written as:

$$u_2^{\mathrm{e}} = u_2^{\mathrm{m}}, \quad \phi^{\mathrm{e}} = \phi^{\mathrm{m}}, \quad \psi^{\mathrm{e}} = \psi^{\mathrm{m}}, \tag{10}$$

$$\tau_{23}^{\mathrm{e}} = \tau_{23}^{\mathrm{m}}, \quad D_3^{\mathrm{e}} = D_3^{\mathrm{m}}, \quad B_3^{\mathrm{e}} = B_3^{\mathrm{m}}. \tag{11}$$

The superscripts "e" and "m" denote quantities related to the PE and PM material, respectively. The upper and lower surfaces of the bilayer system are mechanically free, electrically shorted or open, and magnetically shorted or open. In this study, two cases for the boundary conditions are considered [25]:

Case 1: Mechanically free, electrically open and magnetically shorted surfaces (denoted by "os"), i.e.,

$$\tau_{23}^{\mathrm{e,m}} = D_3^{\mathrm{e,m}} = B_3^{\mathrm{e,m}} = 0. \tag{12}$$

Case 2: Mechanically free, electrically shorted and magnetically open surfaces (denoted by "so"), i.e.,

$$\tau_{23}^{\mathrm{e,m}} = \phi^{\mathrm{e,m}} = \psi^{\mathrm{e,m}} = 0. \tag{13}$$

The first case is the electrically open and magnetically shorted (os), and the second is the electrically shorted and magnetically open case (so) for which the state vector does not keep the same components. Concerning the "os" case, $\xi(z)$ includes the electric displacement D_3 and the magnetic induction B_3. As for the "so" case, $\xi(z)$ includes the electrical potential ϕ and magnetic potential Ψ. Accordingly, two types of (6×6) matrices Q^{os} and Q^{so} are then constructed for the magnetoelectrically open and shorted cases, respectively:

$$\begin{pmatrix} u_2^{\mathrm{e}} \\ \phi^{\mathrm{e}} \\ \psi^{\mathrm{e}} \\ \tau_{23}^{\mathrm{e}} \\ D_3^{\mathrm{e}} \\ B_3^{\mathrm{e}} \end{pmatrix}_0 = \begin{pmatrix} Q_{11}^{\mathrm{os}} & Q_{12}^{\mathrm{os}} \\ Q_{21}^{\mathrm{os}} & Q_{22}^{\mathrm{os}} \end{pmatrix} \begin{pmatrix} u_2^{\mathrm{m}} \\ \phi^{\mathrm{m}} \\ \psi^{\mathrm{m}} \\ \tau_{23}^{\mathrm{m}} \\ D_3^{\mathrm{m}} \\ B_3^{\mathrm{m}} \end{pmatrix}_{-h}, \tag{14}$$

$$\begin{pmatrix} u_2^{\mathrm{e}} \\ D_3^{\mathrm{e}} \\ B_3^{\mathrm{e}} \\ \tau_{23}^{\mathrm{e}} \\ \phi^{\mathrm{e}} \\ \psi^{\mathrm{e}} \end{pmatrix}_0 = \begin{pmatrix} Q_{11}^{\mathrm{so}} & Q_{12}^{\mathrm{so}} \\ Q_{21}^{\mathrm{so}} & Q_{22}^{\mathrm{so}} \end{pmatrix} \begin{pmatrix} u_2^{\mathrm{m}} \\ D_3^{\mathrm{m}} \\ B_3^{\mathrm{m}} \\ \tau_{23}^{\mathrm{m}} \\ \phi^{\mathrm{m}} \\ \psi^{\mathrm{m}} \end{pmatrix}_{-h}. \tag{15}$$

In order to obtain the nontrivial solutions of the above equations (Eqs. (14–15)), the determinant of $Q_{21}^{\mathrm{os,so}}$ must vanish. So, the dispersive behaviors for the magnetoelectrically open and shorted case can be investigated.

4 Numerical results and discussion

4.1 $BaTiO_3/CoFe_2O_4$ layered plate

The investigation is limited to the propagation of the SH waves in the structure consisting of the PM and PE layers. Both materials are hexagonal (6 mm) crystals (transversely isotropic materials). The x_1–x_3-plane is an isotropic plane for both materials. The SH wave propagating in the structure along the x_1-axis possesses only one component of mechanical displacement u_2 accompanied by both electric potential ϕ and magnetic potential Ψ. The origin of the laminate is taken in the lower interface of the bottom layer. As an illustrative example, a two-layered multiferroic laminate with the stacking sequence F/B (B and F denote $BaTiO_3$ and $CoFe_2O_4$, respectively) was investigated in this section. For the sake of comparison, the results of the homogeneous plate made of piezoelectric $BaTiO_3$ (i.e., with a B/B stacking) and piezomagnetic $CoFe_2O_4$ (i.e., with an F/F stacking) are also presented. The material properties are listed in Table 1 [25]. Firstly, to ensure the proper conduct of calculations, we will consider an example taken from literature [25]. In the following figures, the horizontal axis represents the non-dimensional wave number kh, and the vertical axis represents the non-dimensional phase velocity C/C_{sh} where C is the phase velocity of the mode and C_{sh} is the bulk shear wave velocity of the $CoFe_2O_4$. Figure 2 shows the dispersion curves associated with Lamb waves propagating in a bilayer made of PM/PE ($CoFe_2O_4/BaTiO_3$). For validation, a comparison should be made in the case where the plate is assumed to be free of residual stress ($\alpha = 0$). In fact, comparing the result obtained by our method with that obtained by Zhou et al. [26], we find that both dispersion diagrams agree perfectly. In addition, $\varepsilon^0 = 8.8510^{-12}\,\mathrm{Fm}^{-1}$, and $\mu^0 = 4\pi \times 10^{-7}\,\mathrm{Am}^{-1}$ are the dielectric constant and permeability of vacuum, respectively. The dispersion curves of the first five modes for $BaTiO_3/CoFe_2O_4$ coupled plates are shown in Fig. 2a, b with different sequences B/B, F/F, and F/B. Comparing Fig. 3a, b, it can be noticed that all these dispersion curves are very similar to each other. However, differences among them do exist in the different stacking sequences. It is clear from Fig. 3a, b that the phase velocity corresponding only to B (i.e., B/B stacking sequence) is much larger than that corresponding to the other stacking sequences. The slight difference which appears in the dispersion curves for the different stacking sequences is perhaps due to the deviation between

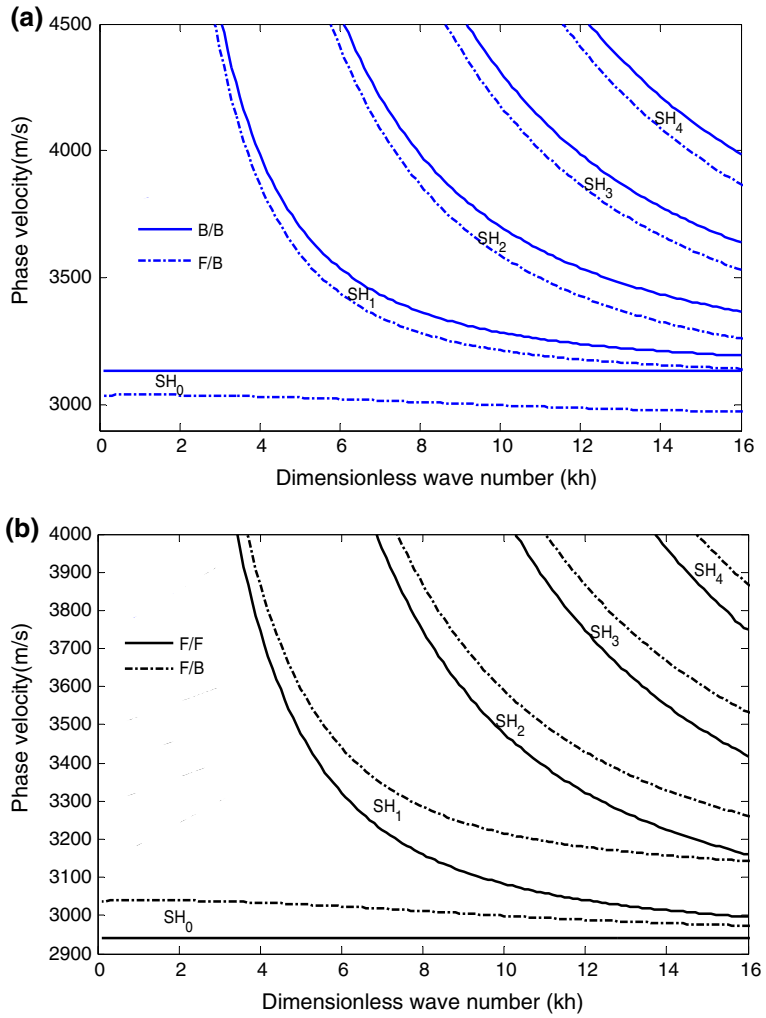

Fig. 3 Dispersion curves of two laminates: **a** B/B and F/B. **b** F/F and F/B sequences

their elastic constants, $BaTiO_3$ seems less stiff than $CoFe_2O_4$, while both of them have nearly the same mass density. Furthermore, the phase velocity approaches the bulk shear wave velocity of the PM material with the increase in the wave number for different modes. It means that the phase velocity approaches the smaller bulk shear wave velocity of the material in the system.

5 Influence of thickness ratio on magneto-electromechanical coupling factor

For SAW devices, not only higher magneto-electromechanical coupling factor, but also less penetration depth of the waves is expected in engineering applications. Either electrically and magnetically open or shorted conditions on the top and bottom surfaces are considered. Using the guiding velocities V_{os} and V_{so}, it is possible to estimate the coefficient of magneto-electromechanical coupling factor K_m^2 for the F/B plate, where V_{os} and V_{so} are the phase velocities for the electrically open and magnetically shorted (os) or electrically shorted and magnetically open (so), respectively. Indeed, as it is thought that it is possible to use the well-known formula used for piezoelectrics, the magneto-electromechanical coupling factor can be evaluated with the following formula [26]:

$$K_m^2 = 2\frac{V_{os} - V_{so}}{V_{os}}. \tag{16}$$

Figure 4 represents the dispersion curves of the fundamental and high-order modes for both "os" and "so" cases of the F/B laminate. As can be seen from this figure, the dispersion curves of the high-order modes of

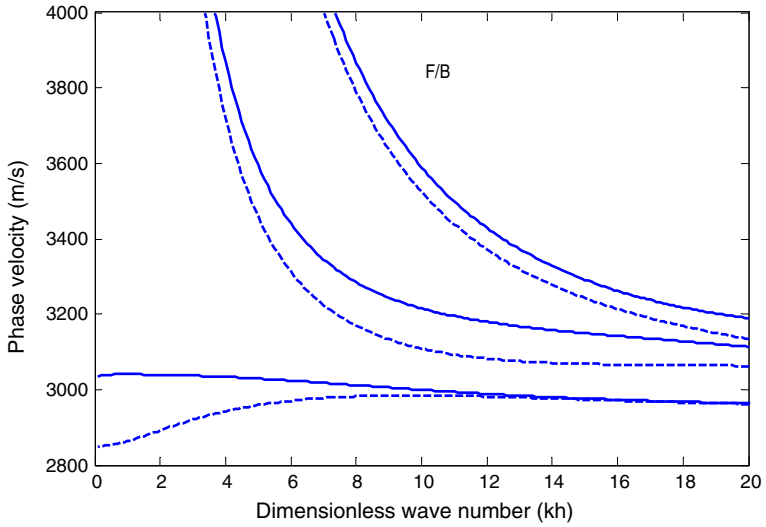

Fig. 4 Dispersion curves of fundamental and high-order modes of F/B plate for "os" and "so" cases circuit ($R = 1$)

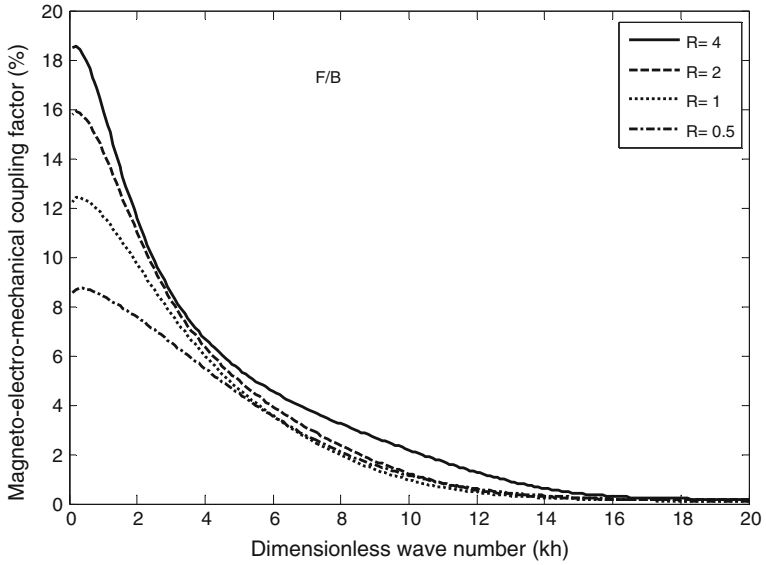

Fig. 5 Effect of thickness ratios on the magneto-electromechanical coupling factor on the first mode

the electrically open case resemble those of the electrically shorted case. But, for the fundamental mode, the discrepancy between phase velocities for both electrically and magnetically open and short cases is significant for low wave number, and then this discrepancy becomes negligible at high wave number range. Hence, in the following discussion, only the electrically open and magnetically shorted case is taken into account. In fact, the detailed discussion will focus on the fundamental mode which is of practical interest. Figure 5 associated with shear wave first mode represents the variation of coefficient of magneto-electromechanical coupling factor, at different thickness ratios ($R = h^{\mathrm{e}}/h^{\mathrm{m}}$). It can be seen that the thickness ratio have remarkable effect on the magneto-electromechanical coupling factor. Actually, the magneto-electromechanical coupling increases with the increase in the thickness ratio. The magneto-electromechanical coupling factor is significant at low kh value and reaches a maximum close to 18% for thickness ratio $R = 4$. This can be explained from Fig. 3b (since the phase velocity corresponding to the B/B stacking sequence is much larger than those corresponding to the other stacking sequences, i.e., F/F or F/B). Actually, when the thickness ratio increases, then the volume fraction of $BaTiO_3$ rises and the dispersion curves approach the B/B stacking sequence. To further illustrate the dispersion behavior, the group velocity V_{g}, which expresses the rate at which energy is transported, is

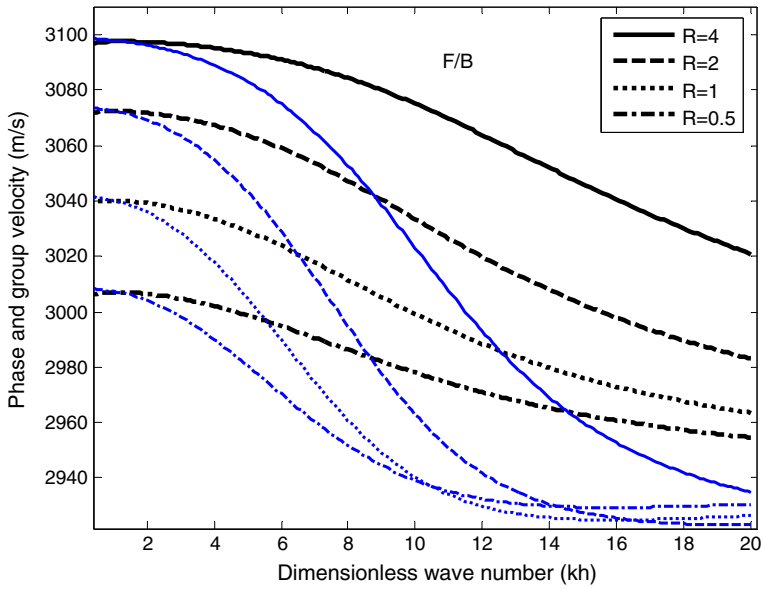

Fig. 6 Effect of thickness ratios on the phase velocity (*thick black line*) and group velocity (*thin blue line*), for "os" case, on the first mode (color figure online)

introduced. The group velocity can be calculated by the following formula [27]:

$$V_{\mathrm{g}} = \frac{\partial \omega}{\partial k} = V_{\varphi} + k\frac{\partial V_{\varphi}}{\partial k}. \tag{17}$$

Figure 6 shows the effect of thickness ratio on the phase and group velocities of the first mode versus kh. It can be seen that the phase velocity starts with C_{SH2} (the shear wave velocity in the PE layer), and as the wave number increases, the phase velocity decreases. Moreover, the phase and group velocities also decrease as the thickness ratio decreases, but when the wave number rises, all the curves converge to C_{SH1} (the shear wave velocity in the PM layer) at high wave number range. This result is quite consistent with Eq. (17) because the phase velocity derivative with respect to kh tends to zero at high wavenumber range, i.e., the group velocity V_{g} tends to the phase velocity V_{φ} which is C_{SH1} for high wave numbers. This effect is due to the fact that the wavelength of the SH waves is comparable to the thickness of the layer for higher ratios. Accordingly, the phase velocities seem sensitive to this parameter thickness ratio. Nevertheless, since the wavelength of the SH waves is smaller than the thickness of the piezomagnetic layer at higher wavenumbers, the PM layer dominates the characteristics of the SH wave propagation.

6 Wave structure analysis

In this section, the modal analysis is performed for a wave propagating in the two-layered multiferroic laminate. Therefore, some physical quantities distributions (normalized) through thicknesses are shown in Fig. 7. The non-dimensional wave number is taken to be $kh = 2$ for SH_0 mode. In this case, the out-of-plane displacement u_2 varies along the thickness direction in a nearly anti-symmetric manner, with respect to the geometric middle surface. Additionally, the component τ_{23} vanishes on the free surfaces, which is compatible with the mechanical boundary conditions. It is noted that the elastic displacement and stress profiles are smooth, but the slope of the electric and magnetic potentials, electric displacement and magnetic induction have a discontinuity across the material interface (say from F to B). Besides, the electric displacement and the electric potential vanish in the upper piezomagnetic layer. Then, the magnetic induction and magnetic potential are insignificant in the lower piezoelectric layer, but not zero. This is due to the fact that we use the general magneto-electric theory; see Eqs. (1, 2, 3), as well as the properties of the materials of Table 1. In such a condition, the electric or magnetic field does not disappear in the phases piezomagnetic or piezoelectric, but they must be small based on the properties of the two materials.

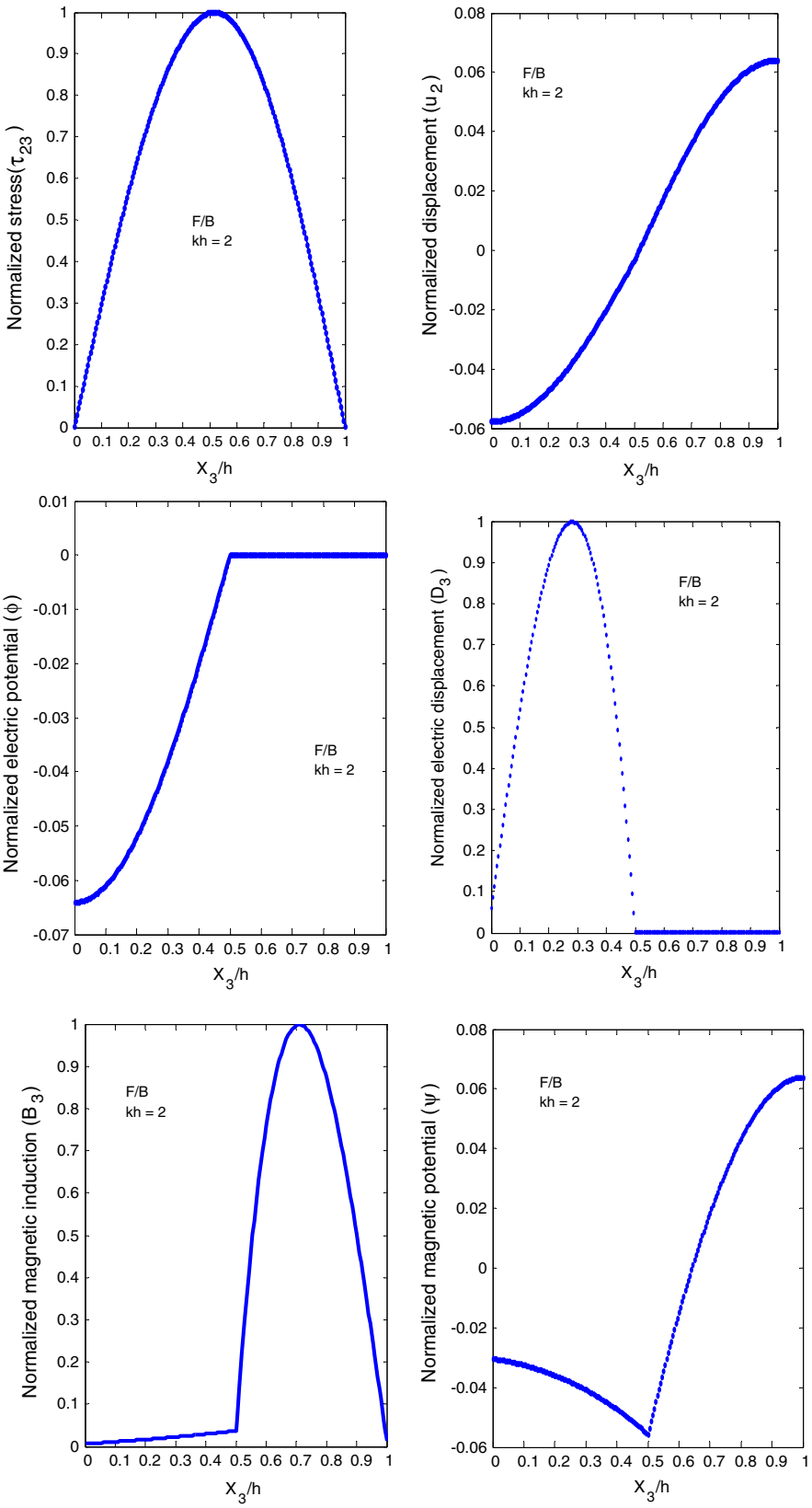

Fig. 7 Distribution of physical quantities in the F/B laminate of SH_0 mode, for "os" case at $kh = 2$

Table 1 Material parameter of piezoelectric and piezomagnetic layer

	$CoFe_2O_4$	$BaTiO_3$
$C_{44}(\times 10^9\,\mathrm{Nm}^{-2})$	45.3	44
$\rho\,(\times 10^3\,\mathrm{kg/m}^3)$	5.3	5.7
$\varepsilon_{ij}\,(\times 10^{-9}\,\mathrm{Fm}^{-1})0.08$	0.08	9.86
$\mu_{11}(\times 10^{-6}\,\mathrm{Ns}^2/\mathrm{C}^2)$	157	5
$e_{15}\,(\mathrm{C/m}^2)$	–	11.4
$h_{15}\,(\mathrm{N/Am})$	550	–
$C_{\mathrm{sh}}\,(\mathrm{m/s})$	2940	3143

7 Conclusion

This paper investigates the propagation behavior of SH waves in a PM/ PE bilayer. The numerical results have shown that the phase velocity approaches the smaller bulk shear wave velocity of the material in the system with the increase in the wave number for different modes. The thickness ratio has a large effect on the phase and group velocities when the wave number is low, and as the wave number increases, the phase velocity decreases. Moreover, the phase and group velocities decrease as the thickness ratio decreases, but when the wave number rises, all these curves converge to the shear wave velocity in the PM layer at high wave number range. Similarl, the magneto-electromechanical coupling factor depends on the thickness ratio; it increases with an increase in the thickness ratio. The magneto-electromechanical coupling factor is significant at low kh value, reaching a maximum of around 18% for thickness ratio $R = 4$. The numerical method as well as the results given in this paper could be useful for the design of the acoustic waves devices based on magnetoelectric materials.

Acknowledgements The authors are grateful for the funding provided to their Laboratory by the Tunisian Ministry of Higher Education and Scientific Research.

References

1. Harshe, G., Dougherty, J.P., Newnham, R.E.: Theoretical modeling of multilayer magnetoelectric composites. Int. J. Appl. Electromagn. Mater. **4**, 145–159 (1993)
2. Nan, C.W.: Magnetoelectric effect in composites of piezoelectric and piezomagnetic phase. Phys. Rev. B **B50**, 6082–6088 (1994)
3. Benveniste, Y.: Magnetoelectric effect in fibrous composites with piezoelectric and piezomagnetic phase. Phys. Rev. B **51**, 16424–16427 (1995)
4. Chen, J., Pan, E., Chen, H.: Wave propagation in magneto-electro-elastic multilayered plates. Int. J. Solids Struct. **44**, 1073–1085 (2007)
5. Thomson, W.T.: Transmission of elastic waves through a stratified solid medium. J. Appl. Phys. **21**, 89–93 (1950)
6. Haskell, N.A.: The dispersion of surface waves on multilayered media. Bull. Seism. Soc. Am. **43**, 17–34 (1953)
7. Gilbert, F., Backus, G.: Propagator matrices in elastic wave and vibration problem. Geophysics **31**, 326–332 (1966)
8. Bahar, L.Y.: A state space approach to elasticity. J. Frankl. Inst. **299**, 33–41 (1975)
9. Pan, E.: Exact solution for simply supported and multilayered magneto-electro-elastic plates. J. Appl. Mech. **68**, 608–618 (2001)
10. Pan, E., Heyliger, P.R.: Free vibrations of simply supported and multilayered magneto-elector-elastic plates. J. Sound Vib. **252**, 429–442 (2002)
11. Ezzin, H., Amor, M.B., Ghozlen, M.H.B.: Love waves propagation in a transversely isotropic piezoelectric layer on a piezomagnetic half-space. Ultrasonics **69**, 83–89 (2016)
12. Jiangong, Y., Juncai, D., Zhijuan, M.: On dispersion relations of waves in multilayered magneto-electro-elastic plates. Appl. Math. Model. **36**, 5780–5791 (2012)
13. Piliposyan, D.: Shear surface waves at the interface of two magneto-electro-elastic media. Multidiscip. Model. Mater. Struct. **8**, 417–426 (2012)
14. Liu, J., Fang, D.-N., Wei, W.-Y., Zhao, X.-F.: Love waves in layered piezoelectric/piezomagnetic structures. J. Sound Vib. **315**, 146–156 (2008)
15. Du, J., Jin, K.X., Wang, J.: Love wave propagation in layered magneto-electro-elastic structures with initial stress. Acta Mech. **192**, 169–189 (2007)
16. Chen, J.Y., Chen, H.L.: Love wave propagation in magneto-electro-elastic multilayered structures. Acta Mater. Compos. Sin. **23**, 181–184 (2006)
17. Chen, J.Y., Pan, E., Chen, H.L.: Wave propagation in magneto-electro-elastic multilayered plates. Int. J. Solids Struct. **44**, 1073–1085 (2007)
18. Wang, Q., Quek, S.T., Varadan, V.K.: Love waves in piezoelectric coupled solid media. Smart Mater Struct. **10**(2), 380–8 (2001)

19. Fan, H., Yang, J.S., Xu, L.M.: Antiplane piezoelectric surface waves over a ceramic half space with an imperfectly bonded layer. IEEE Trans. Ultrason. Ferroelectr. Freq. Contr. **53**(9), 1695–1698 (2006)
20. Ben Salah, I., Wali, Y., Ben Ghozlen, M.H.: Love waves in functionally graded piezoelectric materials by stiffness matrix method. Ultrasonics **51**, 310–316 (2011)
21. Pang, Y., Liu, J.-X., Wang, Y.-S., Zhao, X.-F.: Propagation of Rayleigh-type surface waves in a transversely isotropic piezoelectric layer on a piezomagnetic half-space. J. Appl. Phys. **103**, 074901 (2008)
22. Nie, G., An, Z., Liu, J.: SH-guided waves in layered piezoelectric/piezomagnetic plates. Prog. Nat. Sci. **19**, 811–816 (2009)
23. Rokhlin, S.I., Wang, L.: Ultrasonic waves in layered anisotropic media: characterization of multidirectional composites. Int. J. Solids Struct. **39**, 5529–5545 (2002)
24. Rokhlin, S.I., Wang, L.: Stable recursive algorithm for elastic wave propagation in layered anisotropic media: stiffness matrix method. J. Acoust. Soc. Am. **112**, 822–834 (2002)
25. Zhou, Y.Y., Lü, C.F., Chen, W.Q.: Bulk wave propagation in layered piezomagnetic/piezoelectric plates with initial stresses or interface imperfections. Compos. Struct. **94**, 2736–2745 (2012)
26. Jianke, D., Xian, K., Wang, J.: SH surface acoustic wave propagation in a cylindrically layered piezomagnetic/piezoelectric structure. Ultrasonics **49**, 131–138 (2009)
27. Jian Ke, D.U., XiaoYing, J.I.N., Ji, W.A.N.G.: Love wave propagation in layered magneto-electro-elastic structures. Sci. China Ser. G: Phys. Mech. Astron. **51**, 617–631 (2008)